Susceptibility of Water-Emulsified Extra Virgin Olive Oils to Oxidation

L. Ambrosone*, G. Cinelli, M. Mosca, and A. Ceglie

Consorzio per lo sviluppo dei Sistemi a Grande Interfase (CSGI), Department of Food Technology (DISTAAM), Università del Molise, 86100 Campobasso, Italy

ABSTRACT: The effect of emulsion structure on the susceptibility to oxidation of emulsified olive oils was tested. Olive oil samples were emulsified by adding a certain quantity of water in different ways. The resulting water-in-oil emulsions were then oxidized with UV light. The results revealed that the emulsion structure played a significant role in the oxidation process of emulsified olive oils. A kinetic mechanism is discussed based on the PV determined experimentally. The susceptibility of water-emulsified extra virgin olive oils to oxidation was quantified by means of a dimensionless parameter that displayed a characteristic dependence on the specific surface area of the water dispersed phase.

Paper no. J11017 in *JAOCS 83*, 165–170 (February 2006).

KEY WORDS: Droplet size distribution, emulsified olive oil, emulsion structure, extra virgin olive oil, lipid oxidation, susceptibility.

It is common knowledge that extra virgin olive oil has particular nutritional qualities, largely due to its high content of mononsaturated FA and antioxidants (1,2). Olive oils taken directly from the extraction process and not filtered form a special class characterized by the presence of water and particulate suspensions. Recent studies of these genuine extra virgin olive oils have shown that dispersed particles play a stabilizing role in the oil's shelf life (3,4). This aspect continues to captivate food and biomedical scientists because of reports that diets rich in plant antioxidants are associated with low risks of coronary heart disease and cancer (5).

In a previous paper, we verified that in the absence of solid particles and in the presence of only water, the antioxidant function still takes place (6). To emphasize the link between the oxidation process and the interfacial structure, several water-in-oil emulsions were subjected to different oxidizing conditions (6). The results revealed a good correlation between the measured PV and the surface/volume ratio of the dispersed phase (water). Thus, the structure of the water-in-olive oil emulsion plays a significant role in the oil oxidation process.

Fritsch (7) suggested that the oxidation rate in water-in-oil emulsions occurs at a rate similar to that in bulk oil, because the oil surface is exposed directly to air. On the contrary, McClements and Decker (8) argued that pro-oxidants or antioxidants, located within the water droplets or at the water/oil interface, may influence lipid oxidation in water-in-oil emulsions. Although much attention has been given to the study of lipid oxidation in bulk oil and in oil-in-water emulsions, the oxidative degradation of olive oils in water-in-oil emulsions has received little attention in the literature. In this paper we did not analyze the natural oil as a whole but as samples treated by filtering the particulate solids and adding water under controlled conditions (emulsified oil). Here, the effects of the colloidal properties of water-in-oil emulsions on their susceptibility to oxidation are discussed.

EXPERIMENTAL PROCEDURES

Chemicals. All the chemicals used were reagents of analytical grade of 99.9% purity purchased from Carlo Erba Reagenti (Milan, Italy).

Oil sampling. Olives of mixed cultivars (Cima di Mola, Cima di Bitonto, and others) were picked during the 2001/2002 oil campaign and pressed with a discontinuous process. The oil samples were taken directly from the crusher and treated for 15 min with a N_2 current and then stored at 4°C in 50-mL flasks. In this way, each sample was completely used for the analyses once it was slowly taken back to room temperature. The olive oil was characterized by measuring the PV, total acidity, spectrophotometric indexes, and refractive index, according to the official method recommended by the European Community (9). The results are as follows: total acidity (% oleic acid), 0.36 ± 0.02 (SD of six measurements); PV (meq O_2/kg oil), 10.0 ± 0.6 (SD of six measurements); K_{232}, 1.71 (where K_λ is the specific extinction coefficient at wavelength λ); K_{270}, 0.16; ΔK, –0.001 (where ΔK is $K_{270} - 0.5(K_{266} + K_{274})$; refractive index, 1.4680 ± 0.005 (SD of six measurements). It should be stressed that we were interested in studying the water/oil interface in the oxidation process of emulsified olive oils. Therefore, we measured only the parameters that would define the oxidative state of the oil.

Preparation of water/extra virgin olive oil emulsions. Extra virgin olive oil (about 15 g) was filtered in the presence of anhydrous Na_2SO_4 and then 1.5% (w/w) of distilled water was added. The quantity of water added was chosen by means of a stability test. A number of water-in-oil emulsions were prepared by adding different quantities of distilled water and shaking them for 15 min. The test consisted of a visual determination of the highest water quantity for which no phase separa-

---

*To whom correspondence should be addressed at DISTAAM, Università del Molise, via De Sanctis 86100 Campobasso, Italy.
E-mail: ambroson@unimol.it

tion was observed for at least a week, at 25°C. All emulsions were shaken with an UltraTurrax T8-S8NG (100 W; IKA Labortechnik, Janke & Kunkel, GmbH, Staufen, Germany). Owing to the presence of minor constituents (e.g., tyrosol, hydroxytyrosol), microemulsions might form (10). Since such systems are thermodynamically stable and are not visible to the optical microscope, we verified that all the added water was dispersed in the emulsion droplets by centrifuging an emulsified sample at 2150 × *g* for 30 min. In this way, the quantity of water added was totally recovered, indicating that no appreciable amount of water was dispersed in the microemulsion droplets.

Oxidizing conditions. Aliquots of emulsified oil samples (2.5 g) were put in polyester vessels (40 × 40 × 8 mm) and exposed to UV light ($\lambda = 254$ nm). The lamp power was 30 W and the direction of irradiation was perpendicular to the oil surface. The distance between the lamp and the oil surface was 11.5 cm. This distance was the same for all samples so that this parameter was constant in the oxidation process. All analyses were performed simultaneously on different samples. The measurements were performed on filtered olive oil, olive oil without further treatment (natural oil), and filtered olive oil with 1.5% (w/w) of water that was dispersed under different conditions (emulsified oil). Each sample was exposed to oxidation for different lengths of time, at 25°C. The experimental uncertainty was estimated by calculating the SD of repeated measurements (not less than three).

Optical microscopy. Optical micrographs were obtained by means of an optical microscope (Optech, model B5) connected to a Panasonic video camera (model GP-KR222), at 25°C. To obtain representative results from the microscopic analysis of water-in-oil emulsions, the video-enhanced microscopy technique was used (11). This technique combines the magnification power of a microscope with the digital image acquisition capability of a video camera. A series of images for each sample (9–10 pictures, 1000 objects) was analyzed to extract the droplet size polidispersity, which was estimated by counting the average number of droplets at the different radii in micrographs of a Thoma grating. Image analysis software (Sigma Scan Pro; SPSS Science Software Inc., Chicago, IL), which provides a wide range of analytical features in addition to image enhancement, was used for digitizing the images.

RESULTS AND DISCUSSION

Oxidation profiles. Oil oxidation is a generic term used to describe a complex sequence of chemical reactions that result from the interaction of lipids with active oxygen species. The mechanism of oxidation depends on the reactive species involved and on their physicochemical environment, i.e., the local concentration (12). An emulsion is a heterogeneous system in which the local concentration can vary widely; therefore, the course of the reaction may be modified by modulating the emulsion structure (13).

To verify this idea, we prepared emulsions with the same water content but emulsified by shaking them for 15 and 45 min. Hereafter, these samples are referred to as E_{15} and E_{45}, respectively.

Many factors can affect the oxidation process (14,15). To identify the contribution attributable to the emulsion structure, we compared the results of oil samples that were emulsified in different ways but oxidized under the same conditions. A quantity of filtered oil was divided into three aliquots. One of them was directly oxidized, whereas the others were used to prepare the samples E_{15} and E_{45} and then oxidized.

However, the shaking operation puts the oil in contact with a large amount of air, so the PV value could increase as a result of agitation. For this reason, we decided to check this effect on two virtual samples, E_{15} and E_{45}. These PV were obtained by oxidizing filtered, nonemulsified samples after having shaken them for 15 and 45 min, respectively. Figure 1 compares the PV measured in this condition with those measured in a filtered but nonshaken sample. It is evident that the agitation did not affect the susceptibility of the oil to oxidation.

In addition, the filtering operation might alter the resistance of the oil to oxidation; therefore, a natural oil sample was oxidized as well. As one can see in Figure 2, the measured PV for filtered and natural samples coincided within the experimental error. In other words, the filtered and natural samples showed the same susceptibility to oxidation.

Finally, as shown in Figure 3, we compared the oxidative properties of filtered and natural samples, both emulsified with the same water quantity (1.5% w/w). The results showed no significant difference, implying that there was no synergetic effect between the added water and the particulate that was present in the natural oil.

It follows that the different trend of $\mathrm{PV}^{0.5}$ vs. time displayed by the samples E_{15} and E_{45} (Fig. 4) must be ascribed to the emulsion structure**,** i.e., droplet size distribution of the dispersed phase (water).

Droplet size distribution. In a real emulsion, droplets are polydispersed with respect to their size. Mainly to aid in interpreting the data presented, we have provided some details about size distributions and their characterization (16). Let $N(D)$ be the fraction of droplets with diameter less than D, then $dN/dD = P(D)$ is the size distribution function. Many of its properties can be derived by the moments

$$\mu_n = \int_0^\infty D^n P(D)dD \qquad [1]$$

where n is the moment order. Obviously $\mu_0 = 1$. Any type of average diameter is thus given by

$$D_{nm} = \left(\frac{\mu_n}{\mu_m}\right)^{1/(n-m)} \qquad [2]$$

For instance, D_{10} is the average diameter and D_{32} is the volume/surface ratio or Sauter average.

Polydispersity is best expressed as the relative width of the distribution:

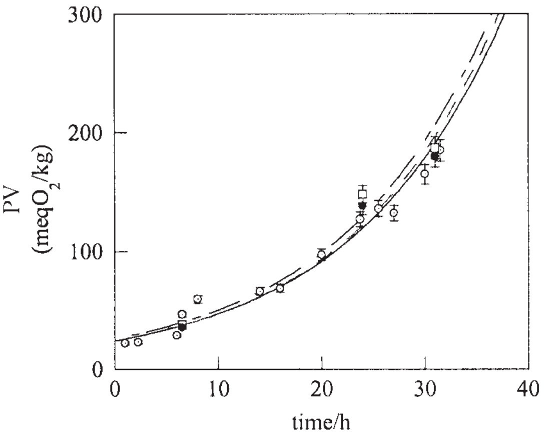

FIG. 1. PV of filtered extra virgin olive oil as a function of UV oxidation time. (□) Shaken for 15 min; (●) shaken for 45 min; (○) directly oxidized. Data shown are the average of triplicate samples, at 25°C. Error bars represent SD ($n \geq 3$).

$$\sigma_n = \sqrt{\frac{\mu_n \mu_{n+2}}{\mu_{n+1}^2} - 1} \qquad [3]$$

Another important parameter is the specific surface area of the dispersed phase:

$$A_D = \frac{6\mu_2}{\mu_3} = \frac{6}{D_{32}} \qquad [4]$$

When the agitation intensity is varied, not only does the average size change but also the relative width of the distribution. Therefore, we monitored the system evolution by measuring the droplet size distribution during the oxidation process. To highlight graphically the changes in the distribution functions, we displayed the results of optical microscopy in 3-D plots (Figs. 5, 6). This representation allowed us to see at a glance the time evolution of droplet distributions; these parameters are displayed in Table 1. The oil samples prepared under the same conditions as E_{15} and E_{45} exhibited no change in the distribution function when stored in the dark. This control was performed on all samples and for all oxidation times. One can thus deduce that changes in the shape of the size distributions and of the related parameters displayed in Table 1 must be attributed to the oxidation process.

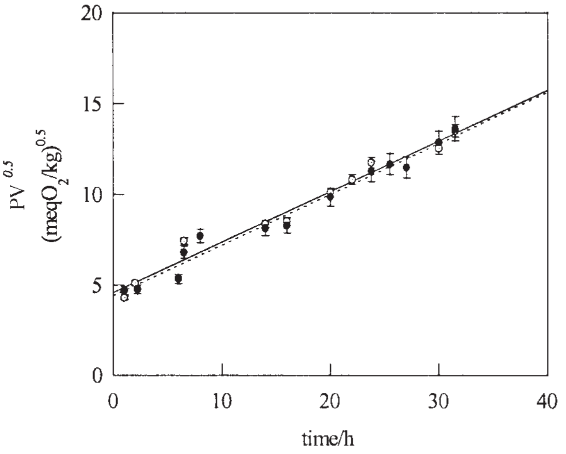

FIG. 2. PV$^{0.5}$ as a function of the UV oxidation time of two different olive oil samples. (○) Natural extra virgin olive oil; (●) filtered extra virgin olive oil. Data shown are the average of triplicate samples, at 25°C. Error bars represent SD ($n \geq 3$).

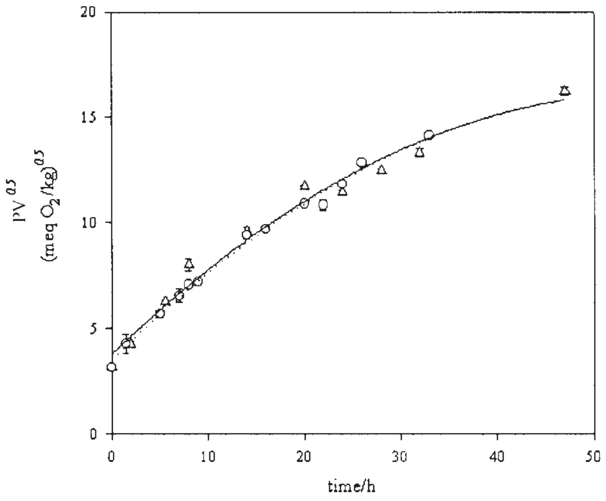

FIG. 3. PV$^{0.5}$ as a function of the UV oxidation time of olive oil samples emulsified with 1.5% (w/w) of distilled water. (●) Filtered extra virgin olive oil; (○) natural extra virgin olive oil. Data shown are the average of triplicate samples, at 25°C. Error bars represent SD ($n \geq 3$).

Oxidation process. An early important observation was that for filtered and natural oil samples, PV$^{0.5}$ vs. time displayed a linear trend (Fig. 2). In agreement with the literature (8,12), this

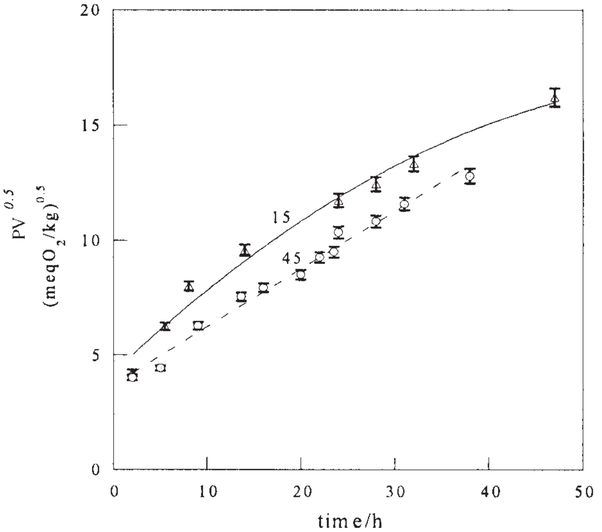

FIG. 4. PV$^{0.5}$ as a function of UV oxidation time of filtered extra virgin olive oil samples emulsified with 1.5% (w/w) of water for different times. The numbers on the curves refer to the emulsifying times. (△) Sample emulsified for 15 min; (○) sample emulsified for 45 min. Data shown are the average of triplicate samples, at 25°C. Error bars represent SD ($n \geq 3$).

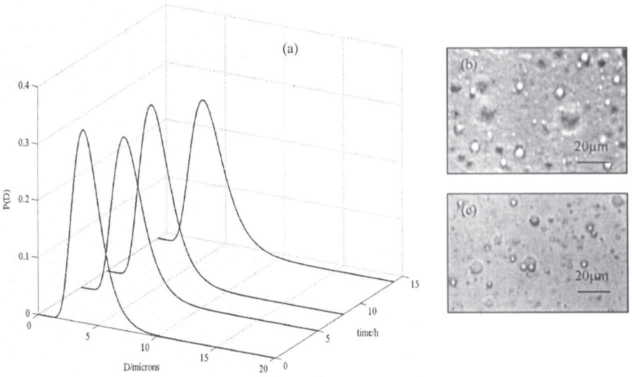

FIG. 5. (a) Droplet size distribution time evolution of filtered extra virgin olive oil emulsified for 45 min (E_{45}). (b, c) Optical microscopy: representative micrographs of the E_{45} emulsion at different oxidation times. Bar = 20 μm. (b) E_{45} just after preparation; (c) E_{45} after 14 h of UV oxidation.

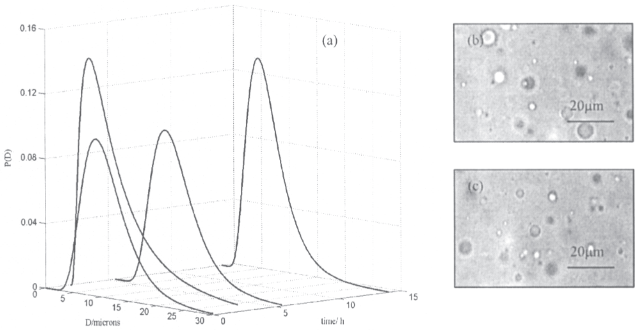

FIG. 6. (a) Droplet size distribution time evolution of filtered extra virgin olive oil emulsified for 15 min (E_{15}). (b, c) Optical microscopy: representative micrographs of the E_{15} emulsion at different oxidation times. Bar = 20 μm. (b) E_{15} just after preparation; (c) E_{15} after 14 h of UV oxidation.

indicates that the initiation step of the oxidation process starts with the removal of hydrogen from the FA molecule, leading to the formation of free radicals and, furthermore, to the formation of hydroperoxides in the propagation step. To understand this point, we can write the propagation steps as follows:

$$R\cdot + O_2 \rightarrow ROO\cdot \quad [5]$$

$$ROO\cdot + RH \rightarrow ROOH + R\cdot \quad [6]$$

where RH is any unsaturated FA, R· is a free radical formed by removing a labile hydrogen from a carbon atom adjacent to a double bond, and ROOH is a hydroperoxide.

The formation rate is given by

$$\frac{d[ROOH]}{dt} = k_p[ROO\cdot][RH] \quad [7]$$

where k_p is the rate constant of the propagation step. Obviously, radical formation terminates when free radicals react with each other. The collision between radicals depends on their concentration and relative size. Therefore, we assume

$$ROO\cdot + ROO\cdot \rightarrow \text{nonradical products} \quad [8]$$

to be the most probable step for the termination reaction whose rate, R_t, is

$$R_t = k_t\,[ROO\cdot]^2 \quad [9]$$

TABLE 1
Moments, Sauter Average, Polydispersity, and Specific Surface Area of E_{15} and E_{45} Emulsions at Different Oxidation Times

E_{15}

Time (h)	μ_1[a] (μm)	μ_2[a] (μm^2)	μ_3[a] (μm^3)	μ_4[a] (μm^4)	D_{32}[b] (μm)	σ_2[c]	A_D[d] (μm^{-1})
0	5.23	32.7	240	2030	0.71	0.71	0.72
2	4.08	25.4	209	2030	8.2	0.43	0.73
5.5	5.62	36.1	263	2150	7.3	0.35	0.92
14	4.32	22.3	135	957	6.0	0.41	0.99

E_{45}

Time (h)	μ_1[a] (μm)	μ_2[a] (μm^2)	μ_3[a] (μm^3)	μ4[a] (μm^4)	D_{32}[b] (μm)	σ_2[c]	A_D[d] (μm^{-1})
0	1.056	2.49	6.34	17.7	2.56	0.29	2.34
5	0.937	2.23	5.92	17.4	2.65	0.33	2.26
8	1.095	2.69	7.35	22.2	2.73	0.33	2.20
14	1.050	2.72	7.98	26.3	2.93	0.36	2.05

[a] μ_n, *n*th moment of droplet size distribution.
[b] D_{32}, surface/volume mean diameter or Sauter diameter.
[c] σ_2, relative width of the distribution function.
[d] A_D, specific surface area of the dispersed phase.

where k_t is the rate constant of the termination step.

Using the matter balance and the steady-state hypothesis, one finds that the initiation rate = termination rate, i.e., $R_i = R_t$, which allows us to transform Equation 7 into

$$\frac{d[ROOH]}{dt} = \left(\frac{k_p}{k_t^{1/2}} [RH] \right) R_i^{1/2} \qquad [10]$$

This equation indicates that for a small extent of reaction, where $[RH] \approx [RH]^0$ (initial concentration), the formation rate of hydroperoxides depends only on the initiation rate.

Nevertheless, the experimental results given in Figure 2 are compatible with Equation 10 only if R_i is proportional to [ROOH]. This suggests that the initiation step is

$$\mathrm{ROOH} + h\nu \rightarrow \text{free radicals} \qquad [11]$$

whereby

$$R_\mathrm{i} = k_\mathrm{i} I[\mathrm{ROOH}] = k_\mathrm{I}[\mathrm{ROOH}] \qquad [12]$$

with I being the radiation intensity.

We can then integrate Equation 10 analytically, obtaining

$$[\mathrm{ROOH}]^{1/2} = PV^{1/2} = PV_0^{1/2} + \left(\frac{k_p^{1/2} k_I^{1/2} [RH]_0}{2 k_t^{1/2}} \right) t \qquad [13]$$

which is the equation fitting the experimental results. We therefore conclude that, in nonemulsified oil, the hydroperoxide formation reaction has a kinetic of the order 0.5. If a certain water quantity is dispersed in the oil, the kinetic order is not preserved, as one can observe in Figure 4. In addition, the different behavior of samples E_{15} and E_{45} cannot be attributed to a direct "chemical action" exerted by the water molecules, as their concentration is the same in all samples. Furthermore, it should be underlined that the kinetic equations discussed here are valid only in the homogeneous phase. On the contrary, in a heterogeneous system the flux through the interfaces may alter the overall kinetic. Thus, a physical action of water droplets on the hydroperoxide concentration is expected. Furthermore, we notice that if in Equation 12 the [ROOH] change is small compared with the overall change, so that $R_i \approx$ constant, then the integration of Equation 10 gives

$$[\mathrm{ROOH}] = [PV] = [PV]_0 + \left(\frac{k_p [RH]_0}{k_t^{1/2}} \right) R_i^{1/2} t \qquad [14]$$

and the hydroperoxide formation reaction exhibits a zero-order kinetic. Moreover, if Equations 13 and 14 describe the experimental curves shown in Figure 4, we can argue that the presence of water molecules is "kinetically" equivalent to a decreasing RH concentration. The water effect must be ascribed to the amphiphilic nature of the hydroperoxide molecules. In fact, even though RH molecules are largely hydrophobic, the intermediates of oil oxidation are quite surface active. An important effect is the capacity of water droplets to act as a "sink" for hydroperoxide molecules, affecting the development of the reaction. In this context, the "interphase" concept, i.e., the imaginary region between the continuous and dispersed phases, is crucial. The interphase characteristics depend on the type and concentration of molecules present, and the fraction of space occupied by this region is linked to the droplet size.

Assuming that the interphase is δ thick, the volume fraction of the interfacial region in the whole emulsion, φ_I, is given by

$$\varphi_I = \frac{\text{interphase volume}}{\text{dispersed phase volume}} \qquad [15]$$

which, in mathematical terms, becomes

$$\varphi_I = 1 - \frac{\int_0^\infty \left(\frac{D}{2} \right)^3 P(D)dD}{\int_0^\infty \left(\frac{D}{2} + \delta \right)^3 P(D)dD} = 1 - \frac{1}{1 + 6\frac{\delta}{D_{32}} + 12\left(\frac{\delta}{D_{31}} \right)^2 + 8\left(\frac{\delta}{D_{30}} \right)^3} \qquad [16]$$

where Equations 1 and 2 have been used.

Generally δ is in the order of a few nanometers thick whereby, using Equation 4, this relationship can be simplified into

$$\varphi_I = \frac{6\delta}{D_{32}} = A_D \delta \qquad [17]$$

It is evident that the volume percentage of the interfacial region is proportional to the specific surface. Consequently, for relatively small droplets (large A_D) the interfacial region comprises a significant volume of the total dispersed phase. A "significant volume fraction" means that some molecules will tend to accumulate in this region, especially if they are present at low concentrations. Hydroperoxides are present in very small quantities and will therefore tend to align themselves so as to better interact with their environment.

The orientation of hydroperoxide molecules at the interfacial region affects the oxidation process because it influences their accessibility during the course of the reaction. Thus, reducing the particle size would be expected to decrease the initiation rate, owing to a larger area of interfacial contact with ROOH molecules. Quantitatively, this implies that the formation rate of hydroperoxides relies on φ_I and, according to Equation 16, on A_D. To quantify this effect, we introduce the dimensionless parameter

$$\chi(t) = \frac{PV(t) - PV_0(t)}{PV_0(t)} \qquad [18]$$

which measures the decreasing or increasing PV of water-in-oil emulsions with respect to the filtered sample assumed as a reference. The susceptibility, χ, which can be determined at any time independently of the system structure, denotes the "oxidative state" of the oil; the term A_D instead measures the "emulsification state" of the oil. Thus, if the oxidation reaction is "surface driven," then χ values for samples emulsified in different ways will be related through A_D. Therefore, we used the experimental results and the data in Table 1 to evaluate χ and A_D for samples E_{15} and E_{45}.

Although data points are not uniformly distributed in the experimental range, they can be fitted with a polynomial of the second degree, within an error of 1% (see Fig. 7). This is strong evidence that both data sets (E_{15} and E_{45}) are expressions of the same physical process involving the water droplets.

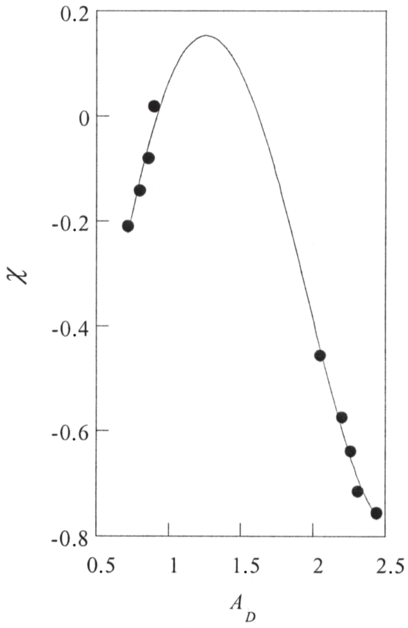

FIG. 7. Susceptibility of all samples to oxidation as a function of the specific surface area of the dispersed phase.

Notwithstanding, during the oxidation reaction the curve $\chi(A_D)$ is not monotone, indicating that the water droplets behave differently. For a small value of A_D, that is, for large volumes of the dispersed phase, the chemical effect of water might gain a certain importance. For the large droplets, the probability then increases of forming hydroxyl radicals from the water molecules. In these conditions water can catalyze the initiation step according to

$$H_2O + h\nu \rightarrow \cdot OH \quad [19]$$

$$RH + \cdot OH \rightarrow R\cdot + H_2O \quad [20]$$

$$ROOH + \cdot OH \rightarrow ROO\cdot + H_2O \quad [21]$$

$$RO\cdot + HO \rightarrow ROOH \quad [22]$$

It is worth noting that the PV trends displayed in Figure 4 and Equations 19–22 depend on the overall water concentration. However, if the water concentration is held constant, the emulsified olive oil shows a susceptibility to oxidation that is a function of the specific surface of the water droplet. This is clear evidence that water droplets play a physical role in the oxidation process. Nevertheless, when the droplet density is high enough, the probability of direct oxidation (for interaction with UV radiation) becomes significant. This dual nature of the water behavior might explain the nonmonotone trend displayed in Figure 7.

More information about the role of the dispersed water can be gathered by studying the oxidation process and evolution of droplet size distribution of olive oils emulsified using different water concentrations.

REFERENCES

1. Tuck, K.L., and P.J. Hayball, Major Phenolic Compounds in Olive Oil: Metabolism and Health Effects, *J. Nutr. Biochem. 13*:636–644 (2002).
2. Papadopulos, G., and D. Boskou, Antioxidant Effect of Natural Phenols on Olive Oil, *J. Am. Oil Chem. Soc. 68*:669–671 (1991).
3. Hoffmann, G., *The Chemistry and Technology of Edible Oils and Fats and Their High Fat Products*, Academic Press, San Diego, 1989, pp. 29–119.
4. Lerker, G., N. Frega, F. Bocci, and G. Servidio, "Veiled" Extra-Virgin Olive Oil: Dispersion Response Related to Oil Quality, *J. Am. Oil Chem. Soc. 71*:657–658 (1994).
5. Kiritsakis, A.K., *Olive Oil* (2nd edn., augmented and revd.), Food and Nutrition Press, Trumbull, CT, 1998.
6. Ambrosone, L., R. Angelico, G. Cinelli, V. Di Lorenzo, and A. Ceglie, The Role of Water in the Oxidation Process of Extra Virgin Olive Oil*s*, *J. Am. Oil Chem. Soc. 79*:577–581 (2002).
7. Fritsch, CW., Lipid Oxidation—The Other Dimension, *INFORM 5*:423–436 (1994).
8. McClements, D.J., and E.A. Decker, Lipid Oxidation in Oil-in-Water Emulsions: Impact of Molecular Environment on Chemical Reactions in Heterogeneous Systems, *J. Food Sci. 65*:1270–1281 (2000).
9. European Community, Regulation 2568/91, *Off. J. Eur. Commun. L.248* (1991).
10. Kalbanov, A., T. Tarara, R. Arlauskas, and J. Weers, Phospholipids as Emulsion Stabilizers. 2. Phase Behavior vs. Emulsion Stability, *J. Colloid Interface Sci. 184*:227–235 (1996).
11. Sæther, Ø., Flocculation and Coalescence in Oil/Water and Water/Oil Emulsions as Studied by Video Enhanced Microscopy, Ph.D. Thesis, University of Bergen, Bergen, Norway, 1999.
12. Frankel, E.N., *Lipid Oxidation*, The Oily Press, Dundee, Scotland, 1998.
13. Evans, D.F., and H. Wennerström, *The Colloidal Domain: Where Physics, Chemistry, and Technology Meet*, VCH, New York, 1994.
14. Georgalaki, M.D., T.G. Sotiroudis, and A. Xenakis, The Presence of Oxidizing Enzyme Activities in Virgin Olive Oil, *J. Am. Oil Chem. Soc. 75*:155–159 (1998).
15. Kiritsakis, A.K., and L.R. Dugan, Study in Photooxidation of Olive Oil, *Ibid. 62*:892–896 (1985).
16. Orr, C., Emulsion Droplet Size Data, in *Encyclopedia of Emulsion Technology*, edited by P. Becher, Marcel Dekker, New York, 1983, Vol. 1, pp. 369–404.

[Received December 22, 2004; accepted November 16, 2005]